iASPP suppresses Gp78-mediated TMCO1 degradation to maintain Ca^{2+} homeostasis and control tumor growth and drug resistance

Shanliang Zheng[a], Dong Zhao[a], Guixue Hou[b], Song Zhao[c,d,e], Wenxin Zhang[a], Xingwen Wang[a], Li Li[f], Liang Lin[b], Tie-Shan Tang[c,d,e], and Ying Hu[a,1]

[a]School of Life Science and Technology, Harbin Institute of Technology, Harbin 150001, China; [b]BGI-SHENZHEN, Shenzhen 518083, China; [c]State Key Laboratory of Membrane Biology, Institute of Zoology, University of Chinese Academy of Sciences, Chinese Academy of Sciences, Beijing 100101, China; [d]Institute for Stem Cell and Regeneration, Chinese Academy of Sciences, Beijing 100101, China; [e]Beijing Institute for Stem Cell and Regenerative Medicine, Beijing 100101, China; and [f]The Third Affiliated Hospital, Harbin Medical University, Harbin 150001, China

Edited by Anjana Rao, Signalling and Gene Expression, La Jolla Institute For Allergy & Immunology, La Jolla, CA; received June 20, 2021; accepted December 21, 2021

Ca^{2+} release from the endoplasmic reticulum (ER) is an essential event in the modulation of Ca^{2+} homeostasis, which is coordinated by multiple biological processes, ranging from cell proliferation to apoptosis. Deregulated Ca^{2+} homeostasis is linked with various cancer hallmarks; thus, uncovering the mechanisms underlying Ca^{2+} homeostasis dynamics may lead to new anticancer treatment strategies. Here, we demonstrate that a reported Ca^{2+}-channel protein TMCO1 (transmembrane and coiled-coil domains 1) is overexpressed in colon cancer tissues at protein levels but not at messenger RNA levels in colon cancer. Further study revealed that TMCO1 is a substrate of ER-associated degradation E3 ligase Gp78. Intriguingly, Gp78-mediated TMCO1 degradation at K186 is under the control of the iASPP (inhibitor of apoptosis-stimulating protein of p53) oncogene. Mechanistically, iASPP robustly reduces ER Ca^{2+} stores, mainly by competitively binding with Gp78 and interfering with Gp78-mediated TMCO1 degradation. A positive correlation between iASPP and TMCO1 proteins is further validated in human colon tissues. Inhibition of iASPP-TMCO1 axis promotes cytosolic Ca^{2+} overload–induced apoptotic cell death, reducing tumor growth both in vitro and in vivo. Thus, iASPP-TMCO1 represents a promising anticancer treatment target by modulating Ca^{2+} homeostasis.

iASPP | TMCO1 | calcium | endoplasmic reticulum | apoptosis

Intracellular calcium (Ca^{2+}) impacts nearly every aspect of cellular life, such as proliferation, apoptosis, differentiation, and migration. As such, it is probably unsurprising that accumulating evidence has connected Ca^{2+} signaling disorders with carcinogenesis and tumor progression (1, 2). Thus, identification of the molecular players involved in Ca^{2+} signaling remodeling may not only improve our understanding of cancer pathology but also provide promising targets for the development of novel anticancer treatment strategies.

To achieve precise control over multiple cellular processes, cells have evolved elegant mechanisms to tightly control Ca^{2+} homeostasis by modulating the flow of Ca^{2+} into and out of cells and organelles (3). This process is integrally and coordinately governed by a complicated system that comprises Ca^{2+} pumps, channels, and exchangers on the endoplasmic reticulum (ER) and plasma membrane (4). As a result, Ca^{2+} concentrations vary wildly across intracellular organelles, with the ER serving as the most important Ca^{2+} store (5). ER Ca^{2+} homeostasis is crucial, as Ca^{2+} release from ER leads to the elevation of cytoplasmic Ca^{2+}, which acts as triggers for Ca^{2+}-dependent events in response to diverse stimuli. For example, the opening of ER channels, such as inositol 1,4,5-trisphosphate (IP3) receptors (IP3Rs) and ryanodine receptors (RyRs), results in passive release of ER Ca^{2+} into the cytosol (6–8), whereas the sarco/ER Ca^{2+}-ATPase (SERCA) pumps refill the ER with Ca^{2+} against the concentration gradient to maintain its high Ca^{2+} content (9). Cells also utilize extracellular Ca^{2+} influx mechanisms to refill the cell's internal stores in response to ER Ca^{2+} depletion through the activation of ER Ca^{2+}-binding protein STIM1 followed by that of Orai1, a plasma membrane Ca^{2+} channel (10, 11). It should also be noted that TMCO1 (transmembrane and coiled-coil domains 1), a highly conserved ER-resident Ca^{2+}-channel protein, has been discovered recently, which provides a distinctive mechanism to maintain Ca^{2+} homeostasis by preventing the overfilling of ER stores with Ca^{2+} through inducing Ca^{2+} release from the ER to the cytosol (12). Changes in the expression of ER-resident IP3R, SERCAs, RyR, or STIM1 have been connected with the initiation or progression of various cancer types, such as melanoma, glioblastoma, colon, prostate, and breast cancers (13–18). Their association with drug resistance and cancer metastasis has been also demonstrated (19–23). Such studies underscore the notion that Ca^{2+} flux across the ER may represent a potential target for anticancer treatment. Concordantly, several SERCA, IP3R, and RyR inhibitors or agonists have been identified that disrupt Ca^{2+} homeostasis efficiently in breast and prostate cancer or glioma cells (16, 24–26). However, unlike above-described ER Ca^{2+} modulators, previous studies on TMCO1 have mainly focused on the genetic variations or mutations of this gene in glaucoma or disorders associated with craniofacial

Significance

Accumulating preclinical and clinical evidence has supported a central role for alterations in Ca^{2+} homeostasis in the development of cancer. TMCO1 protein is an identified Ca^{2+}-channel protein, while its roles in cancer remain obscure. Here, we found that TMCO1 is increased in colon cancer tissues. In addition, it is a substrate of E3 ligase Gp78. Enhanced oncogene iASPP stabilizes TMCO1 by competitively binding with Gp78. Inhibition of iASPP-TMCO1 sensitizes cancer cells' response to Ca^{2+}-induced apoptosis. This study has improved our fundamental understanding of the Ca^{2+} homeostasis in cancer cells. iASPP-TMCO1 axis may present a promising therapeutic target that can combine the conventional drugs to reinforce Ca^{2+}-dependent apoptosis.

Author contributions: Y.H. designed research; S. Zheng, D.Z., G.H., S. Zhao, W.Z., X.W., and L. Li performed research; S. Zheng, D.Z., W.Z., X.W., and L. Li contributed new reagents/analytic tools; S. Zheng, D.Z., G.H., L. Liang, T.-S.T., and Y.H. analyzed data; and Y.H. wrote the paper.

The authors declare no competing interest.

This article is a PNAS Direct Submission.

[1]To whom correspondence may be addressed. Email: huying@hit.edu.cn.

This article contains supporting information online at http://www.pnas.org/lookup/suppl/doi:10.1073/pnas.2111380119/-/DCSupplemental.

Published February 4, 2022.

dysmorphisms, skeletal anomalies, and intellectual disability (27–31). There is little known about the roles of TMCO1 in cancer, and it is not clear how its activity is regulated.

On the other hand, the functions of oncogenes and tumor suppressors in modulating Ca^{2+} homeostasis have increasingly attracted attention (32). The activation of oncogene Bcl-2 or loss of tumor suppressor PTEN has been shown to promote carcinogenesis via their noncanonical function of modulating Ca^{2+} homeostasis. iASPP (Inhibitor of Apoptosis Stimulating Protein of P53) is a well-known p53 inhibitor that binds p53 in the nucleus and represses p53's transcriptional activity to inhibit either apoptosis or senescence in a context-dependent manner (33, 34). Recently, iASPP has been found to be predominately localized in the cytosol in cancer cells, where it stabilizes and activates the master antioxidative transcription factor Nrf2 via a p53-independent mechanism (35). In accordance with its inhibition of apoptosis and senescence and ability to reduce oxidative stress, iASPP has been found to be frequently overexpressed in multiple human cancers, being responsible for drug resistance and the poor prognosis of cancer patients (36–38). However, whether or not the activation of iASPP contributes to the dysregulated Ca^{2+} signaling in cancer has yet remained unexplored.

Here, we not only provide evidence that TMCO1 overexpression (OE) confers tumor growth and apoptosis resistance in colon cancer, rendering it a potential oncogene, but also demonstrate the regulatory mechanisms of TMCO1 through proteasome-induced protein degradation mediated by the well-known ER-associated degradation (ERAD) E3 ligase Gp78. Intriguingly, the activity of Gp78 in regulating TMCO1 is under the control of oncogene iASPP, and thereby we establish a connection between the iASPP oncogene and Gp78/TMCO1-regulated Ca^{2+} homeostasis in a p53- and Nrf2-independent manner. These data suggest that TMCO1 has oncogene activity in colon cancers and highlight the notion that oncogenes influence Ca^{2+} signaling to exert their prooncogenic functions.

Results

TMCO1 Protein Is Increased in Colon Cancers. To understand the roles of the recently identified Ca^{2+}-channel protein TMCO1 in cancer, we first studied the protein levels of TMCO1 via the Clinical Proteomic Tumor Analysis Consortium (CPTAC). By doing so, TMCO1 was found to be dramatically increased across different cancer types, such as breast invasive carcinoma (BRCA), lung adenocarcinoma (LUAD), uterine corpus endometrial carcinoma (UCEC), stomach adenocarcinoma (STAD), and colon adenocarcinoma (COAD) (Fig. 1 *A*, *Upper*). Among those, COAD exhibited the highest expression fold-change (Fig. 1 *A*, *Upper*). The up-regulation of TMCO1 protein was further validated in 40 pairs of colon cancer tissues and their matched adjacent normal controls by Western blot (WB) (Fig. 1*B*). We also found that the increased TMCO1 protein was significantly associated with the advanced stages of colon cancers but not associated with sex and age (Fig. 1 *C* and *D*).

In contrast to protein expression, TMCO1 messenger RNA (mRNA) expression patterns were variable among different types of cancers by analyzing transcriptomic data from The Cancer Genome Atlas. For example, it was significantly increased in BRCA and LUAD but not changed in UCEC, STAD, and COAD (Fig. 1 *A*, *Lower*). Consistently, our RT-PCR results showed no obvious change on TMCO1 mRNA in colon cancers either (Fig. 1*E*). Gene amplification at the TMCO1 locus was associated with the increased TMCO1 mRNA (*SI Appendix*, Fig. S1*A*), and this genetic event was relatively frequently observed in BRCA and LUAD (*SI Appendix*, Fig. S1*B*), which may contribute to the increased TMCO1 expression in these two cancer types. However, in those cancers with no changes on TMCO1 mRNA levels, such as UCEC, STAD, and COAD (Fig. 1*A* and *SI Appendix*, Fig. S1*B*), the posttranslational mechanisms may be involved in regulating TMCO1.

To explore this, we take COAD for further analysis. Consistent with the in vivo results, TMCO1 protein was increased at protein levels but not at mRNA levels (Fig. 1*F*). We also found that proteasome inhibitor MG132, but not lysosome inhibitor chloroquine (CQ), elevated TMCO1 protein expression, suggesting that TMCO1 can be regulated by proteasome degradation (Fig. 1 *G* and *H* and *SI Appendix*, Fig. S1 *C* and *D*). The proteasomal degradation of a target protein is mainly mediated by polyubiquitination (39). In line with this, TMCO1 was found to be polyubiquitinated, as indicated by higher molecular bands/smears in an immunoprecipitation (IP) assay in multiple colon cancer cell lines (Fig. 1*I*). Our data also showed that polyubiquitinated TMCO1 was increased by MG132 (*SI Appendix*, Fig. S1 *E* and *H*) or by introducing increased doses of ubiquitin (*SI Appendix*, Fig. S1 *F* and *H*). Conversely, by using USP2cc, a deubiquitylating enzyme, the polyubiquitinated-TMCO1 signal was significantly decreased (*SI Appendix*, Fig. S1 *G* and *H*). These data suggest that TMCO1 can be regulated by unbiquitin-mediated proteasome degradation.

TMCO1 Is a Substrate of E3 Ligase Gp78. We wondered whether the dysregulated TMCO1 protein turnover contributes to its activation in COAD. To test this, the potential E3 ligase involved in regulating TMCO1 protein stability was first explored. Because TMCO1 is localized at the ER (12), its protein levels were measured after inhibiting the expression of a panel of ER-localized E3 ligases (Gp78, RNF5, RNF185, HRD1, SPFH1, and TMEM129). The results revealed that TMCO1 levels were increased by knocking down (KD) of Gp78, RNF5, or RNF185 but not by KD of HRD1, SPFH1, or TMEM129 (Fig. 2*A* and *SI Appendix*, Fig. S2 *A*–*D*). An IP assay revealed that Gp78 was present in exogenously expressed TMCO1 precipitates, while neither RNF185 nor RNF5 was likely to bind with TMCO1 (Fig. 2*B*). Direct interaction between TMCO1 and Gp78 was further validated in an in vitro IP assay using recombinant proteins (Fig. 2*C*). We therefore reasoned that TMCO1 may be a substrate of Gp78.

In support of this idea, the steady-state levels of TMCO1 protein were decreased by Gp78 OE, and no further reduction was observed upon adding MG132 (Fig. 2*D* and *SI Appendix*, Fig. S2*A*). In addition, wild-type (WT) Gp78, but not an E3 ligase–defective Gp78 mutant (C337/374S, MT), ubiquitinated TMCO1 (Fig. 2*E* and *SI Appendix*, Fig. S2*E*). Furthermore, ubiquitin mutant vectors K0, K48, K29, and K63, which contain arginine substitutions at all lysine residues except the ones at the indicated positions, were used in transfection assays to study Gp78-mediated polyubiquitination of TMCO1. Remarkably, TMCO1 polyubiquitination could be detected in the presence of the K48 plasmid but not K0, K29, or K63 (Fig. 2*F* and *SI Appendix*, Fig. S2 *E* and *F*). Consistent with this, the defective K48R ubiquitin mutant prevented the formation of TMCO1 ubiquitin chains (Fig. 2*F* and *SI Appendix*, Fig. S2*E*). Moreover, small interfering RNA (siRNA)–mediated Gp78 KD almost completely abolished TMCO1 K48-linked ubiquitination (Fig. 2*F* and *SI Appendix*, Fig. S2*E*). Therefore, Gp78 is a major E3 that catalyzes K48-linked ubiquitination of TMCO1.

As a substrate of Gp78, we also wondered which residue in TMCO1 is ubiquitinated. To this end, we applied a commonly used bioinformatic tool. As predicted, K40, K116, K160, K172, and K186 were most likely to be sites that could be modified by ubiquitination (*SI Appendix*, Fig. S2*G*). To validate the bioinformatic results, we generated ubiquitination-defective TMCO1 mutants (K40R, K116R, K160R, K172R, and K186R). A ubiquitination assay was conducted after respectively introducing individual mutant constructs into HT-29 cells. As shown, K186R-TMCO1 largely lost its ability to be ubiquitinated, while

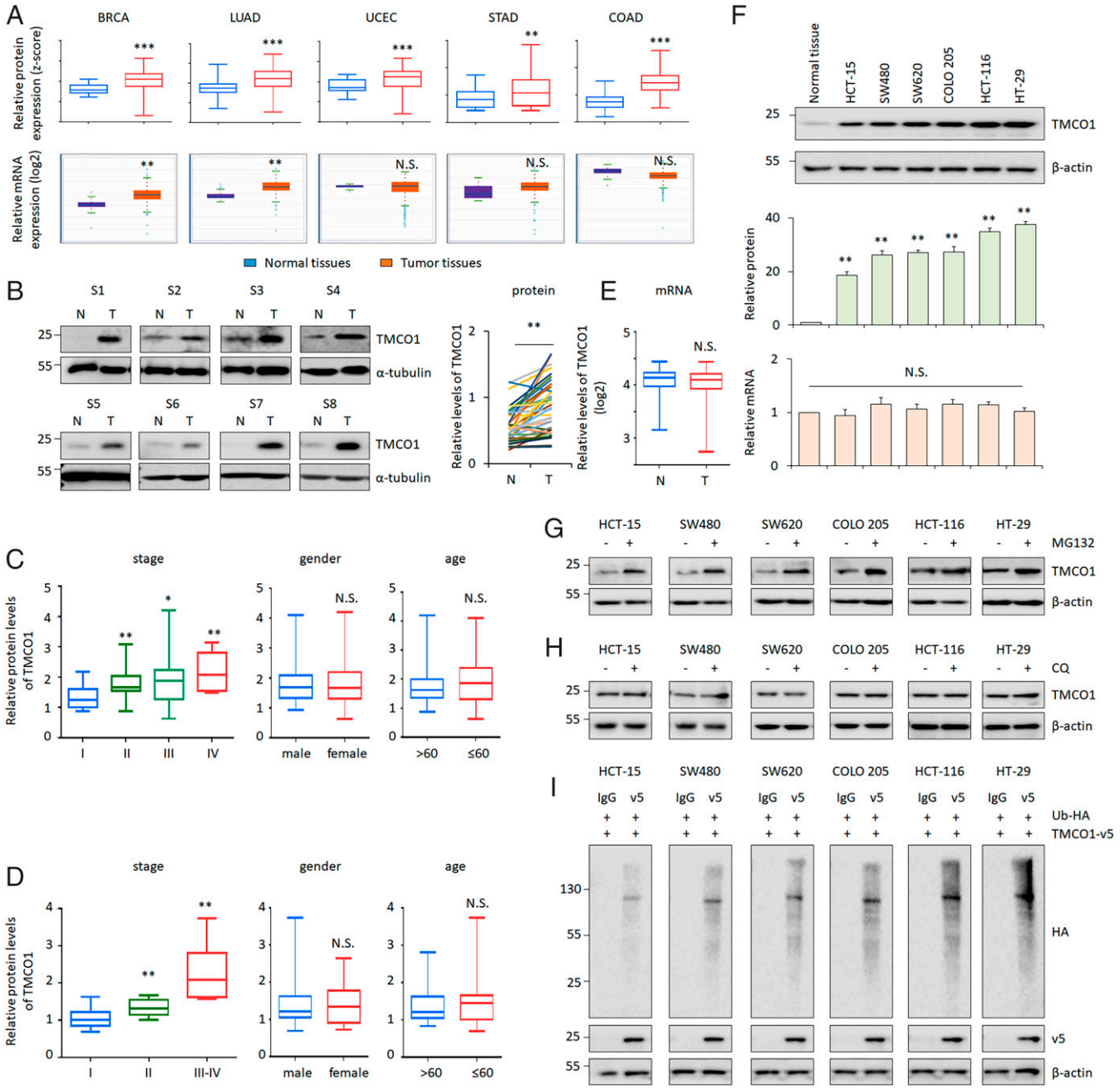

Fig. 1. TMCO1 protein is overexpressed in human colon cancer tissues. (*A* and *B*) TMCO1 protein and mRNA levels were obtained in BRCA, LUAD, UCEC, STAD and COAD, and normal control tissues by analyzing CPTAC (*A*, *Upper*) and The Cancer Genome Atlas (*A*, *Lower*) databases, respectively. Representative WB and quantification of TMCO1 protein expression in 40 pairs of human colon cancer tissues (T) and their matched adjacent normal controls (N) are present in (*B*). α-tubulin was used as a loading control. (*C* and *D*) Correlations between TMCO1 proteins and patients' characteristics (stages, sex, or age) were analyzed using CPTAC dataset (*C*) or WB data derived from *B* (*D*). (*E*) mRNA levels of TMCO1 were detected by qRT-PCR (*E*) in the same set of colon cancer samples described in *B*. (*F*) Representative WB of TMCO1 (*Top*), quantification of TMCO1 protein (*Middle*), and qRT-PCR of TMCO1 mRNA (*Bottom*) in human colon cancer cell lines were present. (*G* and *H*) Representative WB of TMCO1 in colon cancer cell lines after treatment with proteasome inhibitor MG132 (40 μM) (*G*) or lysosome inhibitor CQ (50 μM) (*H*) were determined by WB. β-actin was used as a loading control. (*I*) TMCO1 ubiquitination (Ub-TMCO1) was determined in colon cancer cell lines by IP of anti-v5 followed by WB with anti-HA after transfecting TMCO1-v5 and Ubiquitin (Ub)-HA. β-actin was used as a loading control. Data are derived from three independent experiments and represented as mean ± SEM in the bar graph shown in *F* and *SI Appendix*, Fig. S1 *C* and *D*. The quantification of TMCO1 was analyzed by image J. Values in the control or HT-29 cells were normalized to 1. **P* < 0.05; ***P* < 0.01; ****P* < 0.001; N.S., not significant (*A*–*F*).

other mutants were ubiquitinated to similar extents as WT TMCO1 (Fig. 2*G* and *SI Appendix*, Fig. S2*E*). Cycloheximide (CHX) is widely used to inhibit protein synthesis in eukaryotic cells. Following CHX treatment, the half-life of TMCO1 was determined to be 4 h in control cells, while the half-life of K186R-TMCO1 was much longer than that of its WT counterpart (Fig. 2*H*), and Gp78 expression failed to reduce the levels of K186R-TMCO1 (Fig. 2*I* and *SI Appendix*, Fig. S2*H*). Therefore, Gp78 catalyzes the polyubiquitination of TMCO1 at K186, leading to its ubiquitin-mediated proteasome degradation.

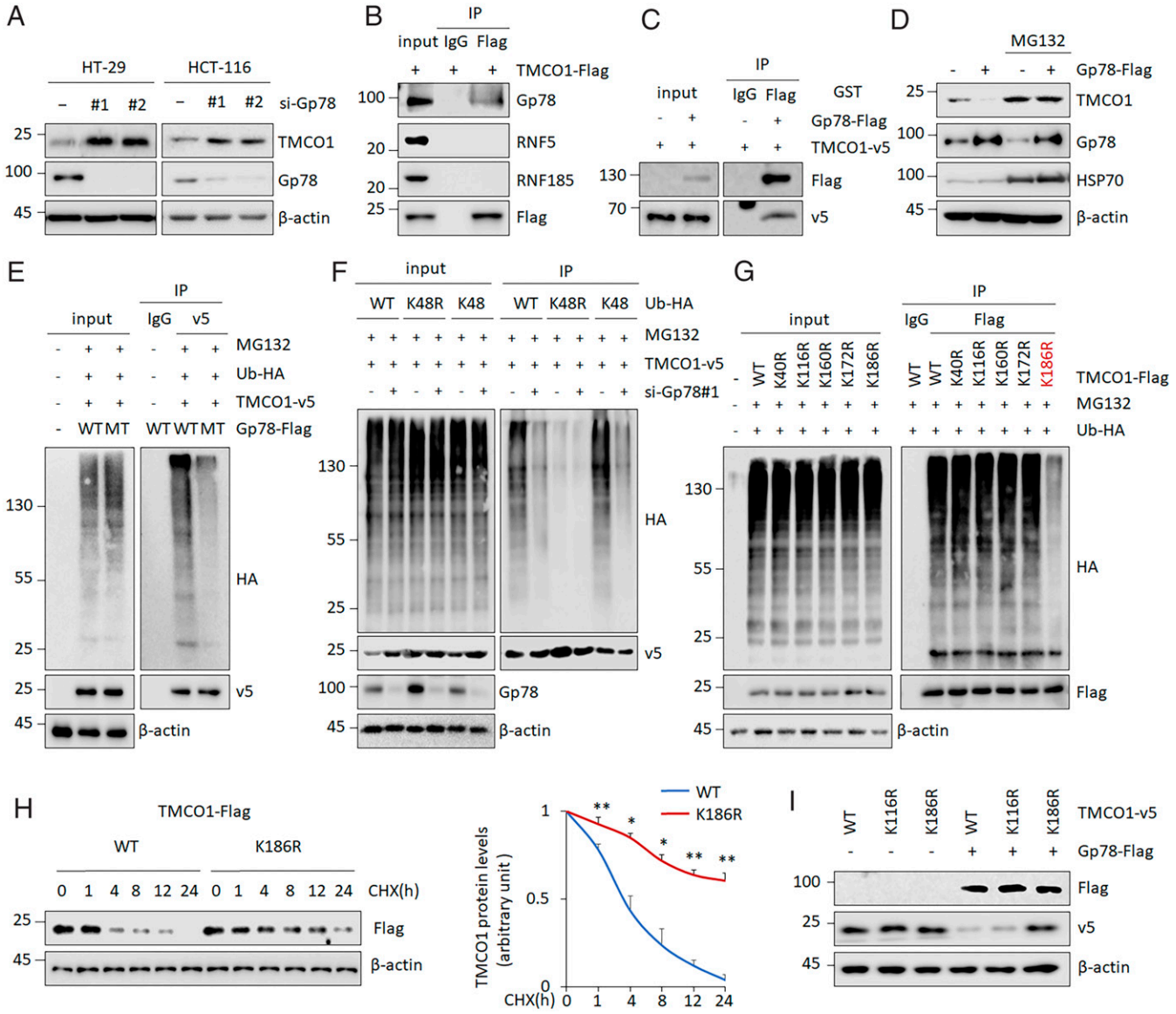

Fig. 2. TMCO1 is a substrate of Gp78. (*A*) Representative WB images were determined by WB after Gp78 KD in HT-29 and HCT-116 cells. β-actin was used as a loading control. (*B* and *C*) The interactions between TMCO1 and candidate E3 ligases, Gp78, RNF5, and RNF185 were analyzed by IP assays in HT-29 cells (*B*). The direct binding between TMCO1 and GP78 was determined by an in vitro IP using purified proteins (*C*). (*D*) TMCO1 protein levels were detected by WB after Gp78 OE in the presence or absence of proteasome inhibitor MG132 (40 μM). HSP70 was used as an E3 ligase–regulated protein control and β-actin was used as a loading control. (*E–G*) Ub-TMCO1 was determined by IP/WB in HT-29 cells overexpressing WT Gp78-Flag or E3 ligase–defective mutant (MT), C337/374S Gp78-Flag (*E*), in cells overexpressing WT or mutant (K48, K48R) Ubiquitin (Ub)-HA in combination with Gp78 KD (*F*), or in cells overexpressing WT TMCO1 or TMCO1 with mutations at the predicted ubiquitination sites (*G*) in the presence of MG132 (20 μM). (*H*) Representative WB (*Left*) and quantification (*Right*) of Flag-tagged TMCO1 (WT and K186R) protein in the presence of 100 μg/mL CHX for the indicated time periods in HT-29 cells. β-actin was used as a loading control. Flag-tagged TMCO1 levels in the untreated cells were normalized to 1. (*I*) The Flag-tagged TMCO1 (WT, K116R, and K186R) levels were evaluated and quantified by WB and imageJ after ectopic Gp78 expression in HT-29 cells. β-actin was used as a loading control. Data are derived from three independent experiments and represented as mean ± SEM in the bar graph (*A*, *D*, *E–G*, and *I*). Quantification data are shown in *SI Appendix*, Fig. S2 *A*, *E*, and *H*). Values in the WT controls were normalized to 1. $*P < 0.05$; $**P < 0.01$ (*H*).

Oncogene iASPP and TMCO1 Are Associated with Each Other In Vivo in Colon Cancer Tissues. We then reasoned that Gp78 dysregulation may the determinant of TMCO1 expression in COAD in vivo. However, it is unlikely the case because Gp78 protein was found to be comparable in COAD and normal controls by analyzing CPTAC samples (*SI Appendix*, Fig. S3*A*). Further analysis also showed that there were no obvious differences in the expression levels of Gp78 in colon cancer specimens versus the paired adjacent normal controls by WB ($n = 40$ pairs) (Fig. 3 *A* and *B*). No obvious correlation between Gp78 and TMCO1 was detected either (Fig. 3*C*). Thus, it is plausible that additional levels of regulation by oncogene or tumor suppressor may exist to determine the activity of Gp78 in regulating TMCO1 in vivo.

To explore this, we analyzed Gp78-interacting proteins using a mass spectrum approach following anti-Gp78 pull-down. As expected, we identified Gp78 itself and the well-known Gp78-binding protein CP3A4 as specific components in the anti-Gp78 immunoprecipitants. TMCO1-specific peptides were also detected. Intriguingly, a well-known oncogene, namely

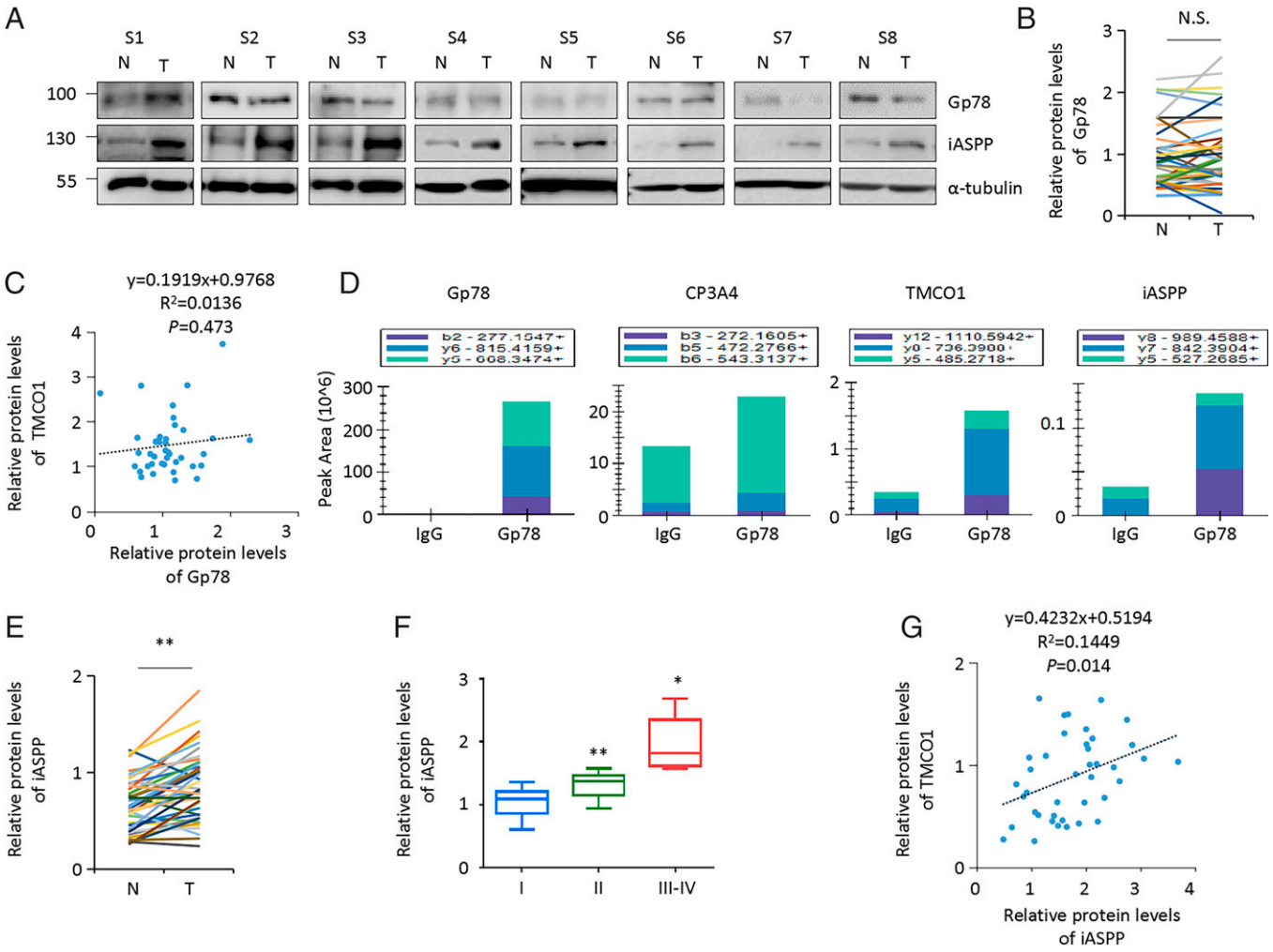

Fig. 3. Oncogene iASPP and TMCO1 are associated with each other in vivo in colon cancer tissues. (*A* and *B*) Representative WB of Gp78 and iASPP proteins in the same set of colon cancer tissues described in Fig. 1*B* were presented. α-tubulin was used as a loading control (same as the blots shown in Fig. 1*B*). (*C*) The scatter diagram showed the lineal correlation of TMCO1/Gp78 ($P = 0.473$, *C*) in colon cancer tissues. (*D*) The key proteins that bind with Gp78 was identified by mass spectrum assay following Gp-78 pull-down. After that, the top three fragments of identified peptides derived from the target proteins (Gp78, CP3A4, TMCO1, and iASPP) were used for quantification. (*E*) Quantification of iASPP WB bands in tumor (T) and the paired normal control (N) were shown in the plot. (*F*) The correlation between iASPP protein levels and tumor stages was shown in the box plot. (*G*) The scatter diagram showed the lineal correlation of TMCO1/iASPP ($P = 0.014$) in colon cancer tissues. N.S., not significant; $*P < 0.05$; $**P < 0.01$ (*B*, *E*, and *F*).

iASPP, was found to be among the significant hits (Fig. 3*D* and *SI Appendix*, Fig. S3*B*). This attracted our attention because iASPP has been shown to be overexpressed in multiple cancers, including COAD (35, 40–42), and our data also revealed that iASPP was increased in colon cancer tissues compared with matched adjacent normal controls (Fig. 3*E*). Like TMCO1, iASPP expression was correlated with advanced stages of colon cancer (Fig. 3*F*). In addition, the fold increase of TMCO1 was positively correlated with that of iASPP (Fig. 3*G*), indicating that iASPP expression is associated with TMCO1 expression in vivo.

iASPP Protects TMCO1 from Ubiquitin–Proteasome Degradation. The next question is whether or not iASPP causes TMCO1 up-regulation. To this end, the levels of TMCO1 were examined after iASPP OE or KD in colon cancer cell lines. Remarkably, TMCO1 was consistently and dramatically increased by iASPP OE and decreased by iASPP KD (Fig. 4*A*). This is likely specific because the expression levels of other ER-resident Ca^{2+} modulators, such as IP3R1, RyR2, SERCA2, and STIM1, were not changed by iASPP expression (Fig. 4*A*). In addition, we found no effect of iASPP on TMCO1 mRNA expression (Fig. 4*A*), while MG132 but not CQ completely rescued iASPP KD–caused TMCO1 repression (Fig. 4*B* and *SI Appendix*, Fig. S4*A*). Compared with the half-life at 4 h in the controls, iASPP-overexpressing cells showed a prolonged half-life at ∼12 h, and iASPP KD cells exhibited a shortened half-life at ∼1 h (Fig. 4 *C* and *D*). Furthermore, iASPP OE inhibited TMCO1 polyubiquitination, while iASPP KD increased it (Fig. 4 *E* and *F*). These data collectively suggest that oncogene iASPP protects TMCO1 from ubiquitin-mediated proteasome degradation.

The Effect of iASPP on TMCO1 Protein Stability Is Dependent on Gp78. We next asked how iASPP inhibits TMCO1 protein turnover. p53 and Nrf2 are the best-known mediators of iASPP functions; however, we observed that the effect of iASPP in regulating TMCO1 was p53- and Nrf2-independent (*SI Appendix*, Fig. S4*B*). In contrast, iASPP-regulated TMCO1 expression was completely abrogated by Gp78 KD (Fig. 4*G* and *SI Appendix*, Fig. S4*C*). This was not due to changes in iASPP protein itself because Gp78 KD produced no obvious effect on iASPP expression (Fig. 4*G* and *SI Appendix*, Fig. S4*C*). In addition, ubiquitination-defective TMCO1 K186R was highly resistant to

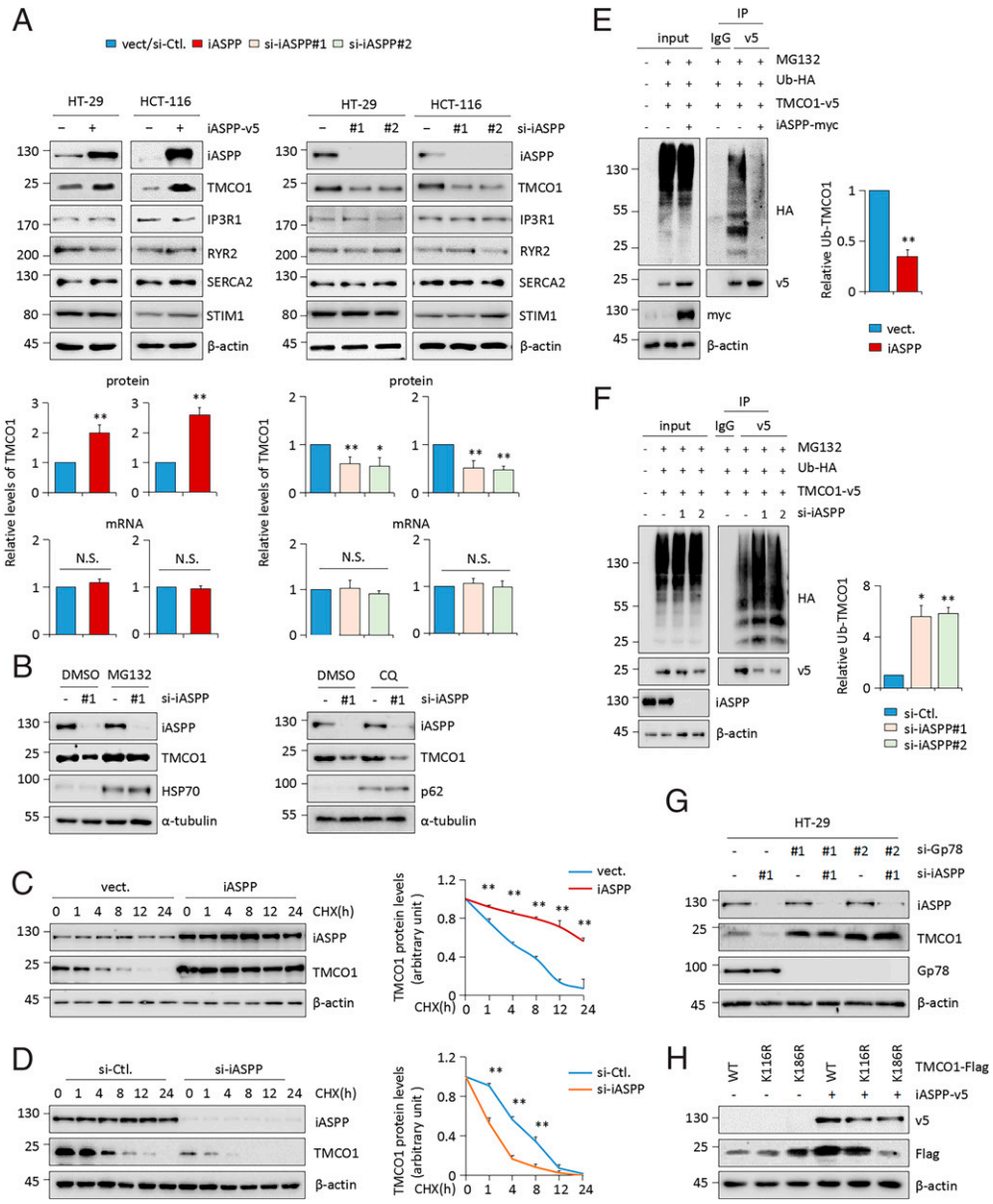

Fig. 4. iASPP protects TMCO1 from ubiquitin-mediated proteasome degradation. (*A*) TMCO1 protein and mRNA levels were determined by WB and qRT-PCR, respectively, after iASPP OE or KD in HT-29 and HCT-116 cells. WB bands of TMCO1 were quantified by Image J and the data were present in the bar graph. (*B*) TMCO1 protein levels were determined by WB after iASPP KD in the presence or absence of proteasome inhibitor MG132 (40 μM) or lysosome inhibitor CQ (50 μM) in HT-29 cells. α-tubulin was used as a loading control. (*C* and *D*) Representative WB and quantification of TMCO1 protein after iASPP OE (*C*) or KD (*D*) in HT-29 cells in the presence of 100 μg/mL CHX at the indicated time periods. TMCO1 levels in the untreated cells were normalized to 1. (*E* and *F*) Ub-TMCO1 was determined by IP of anti-v5 followed by WB with anti-HA after transfecting TMCO1-v5 and Ub-HA in iASPP OE (*E*) and KD (*F*) HT-29 cells in the presence of MG132 (20 μM). β-actin was used as a loading control. The blots of Ub-TMCO1 were analyzed by image J. Values in control cells were normalized to 1. (*G*, *H*) Endogenous TMCO1 levels were determined by WB after iASPP KD and/or Gp78 KD (*G*). The Flag-tagged TMCO1 (WT, K116R, a ubiquitination irrelevance mutant, and K186R, a key ubiquitination defective mutant) levels were evaluated by WB after ectopic iASPP OE in HT-29 cells (*H*). The TMCO1-ub bands were quantified by imageJ. β-actin was used as a loading control. The data derived from three independent experiments are presented as mean ± SEM in the bar graphs (*A*, *E*, and *F*) (quantification data for *B*, *G*, and *H* are shown in *SI Appendix*, Fig. S4 *A* and *C*) or line graphs (*C* and *D*). *$P < 0.05$; **$P < 0.01$; N.S., not significant (*A*, *C*, *D*, *E*, *F*, and *H*).

iASPP-mediated TMCO1 increase when compared with WT TMCO1 or a ubiquitination-site–irrelevant TMCO1 mutant (K116R) (Fig. 4*H* and *SI Appendix*, Fig. S4*C*). Therefore, iASPP stabilizes TMCO1 in a Gp78-dependent manner.

iASPP Stabilizes TMCO1 by Competitively Binding with Gp78. We further explored the underlying mechanism by which iASPP inhibits Gp78-mediated TMCO1 degradation. For this purpose, the effects of iASPP on the expression of Gp78 were first examined. However, Gp78 levels did not change with iASPP expression or KD (*SI Appendix*, Fig. S5*A*). Of interest, we observed that the Gp78, TMCO1, and iASPP forms complex (Fig. 5*A*), which is in line with our mass spectrum results (Fig. 3*D*). In addition, the binding between Gp78 and TMCO1 was decreased with iASPP OE (Fig. 5*A* and *SI Appendix*, Fig. S5*B*). It is thus logical to propose that iASPP may act by inhibiting the binding between Gp78 and TMCO1. If this is the case, iASPP may physically associate with either Gp78 or TMCO1. To test this idea, an in vitro binding assay was applied using in vitro–translated or recombinant proteins of iASPP, Gp78,

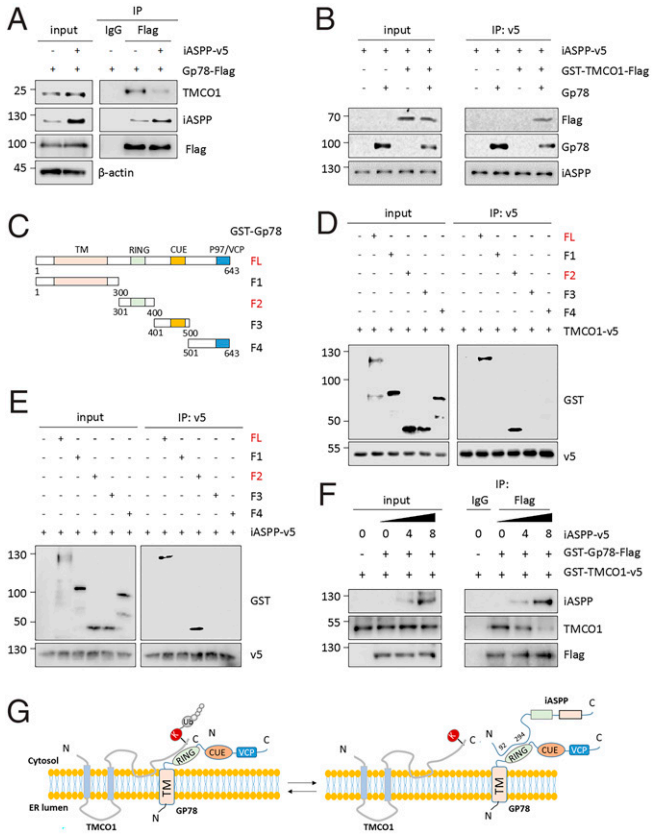

Fig. 5. iASPP stabilizes TMCO1 by competitively binding with Gp78. (*A*) The binding between Gp78 and TMCO1 was compared by IP after iASPP OE. (*B*) The binding among the purified TMCO1 and Gp78 protein and in vitro translated iASPP protein were determined by an in vitro IP assay. (*C–F*) The interactions of full-length (FL) Gp78 or Gp78 truncates, as indicated in the diagram (*C*), with TMCO1 (*D*) or iASPP (*E*), and the interaction among Gp78, iASPP, and TMCO1 (*F*) with increasing dose of iASPP protein (0, 4, and 8 μL) were evaluated by an in vitro IP assay. (*G*) A model proposed on the binding mechanisms of TMCO1/Gp78 and iASPP/Gp78. The representative images derived from three independent experiments. The WB bands (*A* and *F*) were quantified by Image J and presented as mean ± SEM in the bar graphs shown in the *SI Appendix*, Fig. S5 *B* and *D*, respectively.

and TMCO1. The results showed that iASPP was coprecipitated with Gp78, while its interaction with TMCO1 was only observed when Gp78 was present in the mixture (Fig. 5*B*). Therefore, iASPP directly interacts with Gp78 but not TMCO1.

Considering its ability to directly bind with Gp78, we reasoned that iASPP reduces TMCO1/Gp78 interaction possibly by competing with TMCO1 in binding with Gp78. To test this possibility, the binding mechanisms of iASPP/Gp78 and TMCO1/Gp78 were explored. We generated four Gp78-truncated mutants, as depicted in Fig. 5*C*. An in vitro binding assay with an anti-v5 tag antibody revealed that v5-tagged TMCO1 coimmunoprecipitated with WT- and F2(301–400)-Gp78, both containing the Ring domain, but not others, suggesting that the Ring domain is essential for Gp78's binding with TMCO1 (Fig. 5*D*). To better understand which TMCO1 domains contribute to the interaction with Gp78, Gp78 was coexpressed with Flag-tagged forms of full-length, C-, or N-terminal–truncated TMCO1 mutants in HeLa cells. The IP assay revealed that Gp78 coimmunoprecipitated with WT and C-terminal (90–188) TMCO1 but not the N terminus (1–89) (*SI Appendix*, Fig. S5*C*). Therefore, TMCO1 binds with Gp78 through its residues mapped to the C terminus (90–188).

Interestingly, using an in vitro IP assay we found that (301–400) Gp78, the region identified to bind with TMCO1, also contributes to its binding with iASPP (Fig. 5*E*), further supporting the hypothesis that iASPP competes with TMCO1 in binding with Gp78. To provide more direct evidence, the binding between TMCO1 and Gp78 was compared in the presence of increasing amounts of iASPP protein. Indeed, the interaction between TMCO1 and Gp78 gradually decreased with increased binding of iASPP with Gp78 (Fig. 5*F* and *SI Appendix*, Fig. S5*D*). Meanwhile, our results revealed the key residue in (92–294) iASPP that is required for its interaction with Gp78 (*SI Appendix*, Fig. S5*E*), whereas the featured domain in the C terminus of iASPP is unlikely to contribute to its binding with Gp78 (*SI Appendix*, Fig. S5*E*). These data together suggest that iASPP competes with TMCO1 to bind with (301–400) Gp78, leading to increased TMCO1 stability (Fig. 5*G*).

A Function of iASPP to Modulate ER Ca^{2+} Stores by Stabilizing TMCO1. Given that TMCO1 is a Ca^{2+}-channel protein and the function of iASPP in regulating TMCO1, we further investigated iASPP's activity in regulating Ca^{2+} homeostasis. To this end, we measured Ca^{2+} flux in HT-29 and HCT-116 cells grown under Ca^{2+}-free conditions in the presence of ionomycin. Ionomycin was expected to permeabilize the membrane of the stores to Ca^{2+}, causing rapid Ca^{2+} leak. Because the experiments were conducted in the absence of extracellular Ca^{2+}, Ca^{2+} influx through cell membrane was prevented, and therefore detected cytosolic Ca^{2+} flux indirectly reflects Ca^{2+} content in the ER. Under such conditions, the signal of cytosolic Ca^{2+}, as quantified by the area under the curve (AUC), was evident after ionomycin loading. Remarkably, iASPP OE significantly reduced AUC compared with the corresponding controls (Fig. 6 *A* and *B*), whereas iASPP KD enhanced it (Fig. 6 *C* and *D*). The impact of iASPP on ER Ca^{2+} content was confirmed by ionomycin addition after Thapsigargin (TG)–induced Ca^{2+} transient (*SI Appendix*, Fig. S6*A*). Therefore, iASPP reduces ER Ca^{2+} stores.

In addition, we confirmed that TMCO1 KD led to an increased level of Ca^{2+} flux by monitoring cytosolic Ca^{2+} after ionomycin treatment (Fig. 6 *E* and *F*). By contrast, TMCO1 OE reduced Ca^{2+} content at ER (*SI Appendix*, Fig. S6*B*). In addition, endogenous TMCO1 levels were negatively associated with ER Ca^{2+} content by analysis of four representative colon cancer cells with different TMCO1 levels (*SI Appendix*, Fig. S6*C*). TMCO1 OE also reduced Ca^{2+} content at the ER in nonmalignant HEK293T cells (*SI Appendix*, Fig. S6*D*), suggesting this activity of TMCO1 is common. The dependency of iASPP on TMCO1-regulated Ca^{2+} release from the ER was further validated (Fig. 6 *E* and *F*). The results show that the effect of iASPP on ionomycin-induced Ca^{2+} responses was completely abolished by TMCO1 KD (Fig. 6 *E* and *F*). Similar to iASPP, Gp78 was also found to regulate Ca^{2+} flux in a TMCO1-dependent manner (*SI Appendix*, Fig. S6*E*). Also notably, iASPP KD elevated the AUC compared with corresponding controls in p53 null H1299 cells (*SI Appendix*, Fig. S6*F*). Restoring p53 expression in H1299 cells increased ER Ca^{2+} content; however, it has no obvious impacts on the effect of iASPP OE (*SI Appendix*, Fig. S6*G*). Despite observing increased Ca^{2+} release after Nrf2 KD, the ability of iASPP to regulate Ca^{2+} flux was not changed significantly in Nrf2 KD cells (*SI Appendix*, Fig. S6*H*). These data are in line with our finding that iASPP regulates TMCO1 in a p53- and Nrf2-independent manner and further supports the idea that iASPP regulates Ca^{2+} homeostasis mainly by controlling the protein levels of TMCO1.

iASPP-TMCO1 Promote Tumor Growth Both In Vitro and In Vivo. Considering the close association between iASPP and TMCO1 both in vitro and in vivo and the pivotal roles of Ca^{2+} homeostasis in carcinogenesis, we sought to explore the activity of the identified iASPP-TMCO1 axis on tumor growth. As shown,

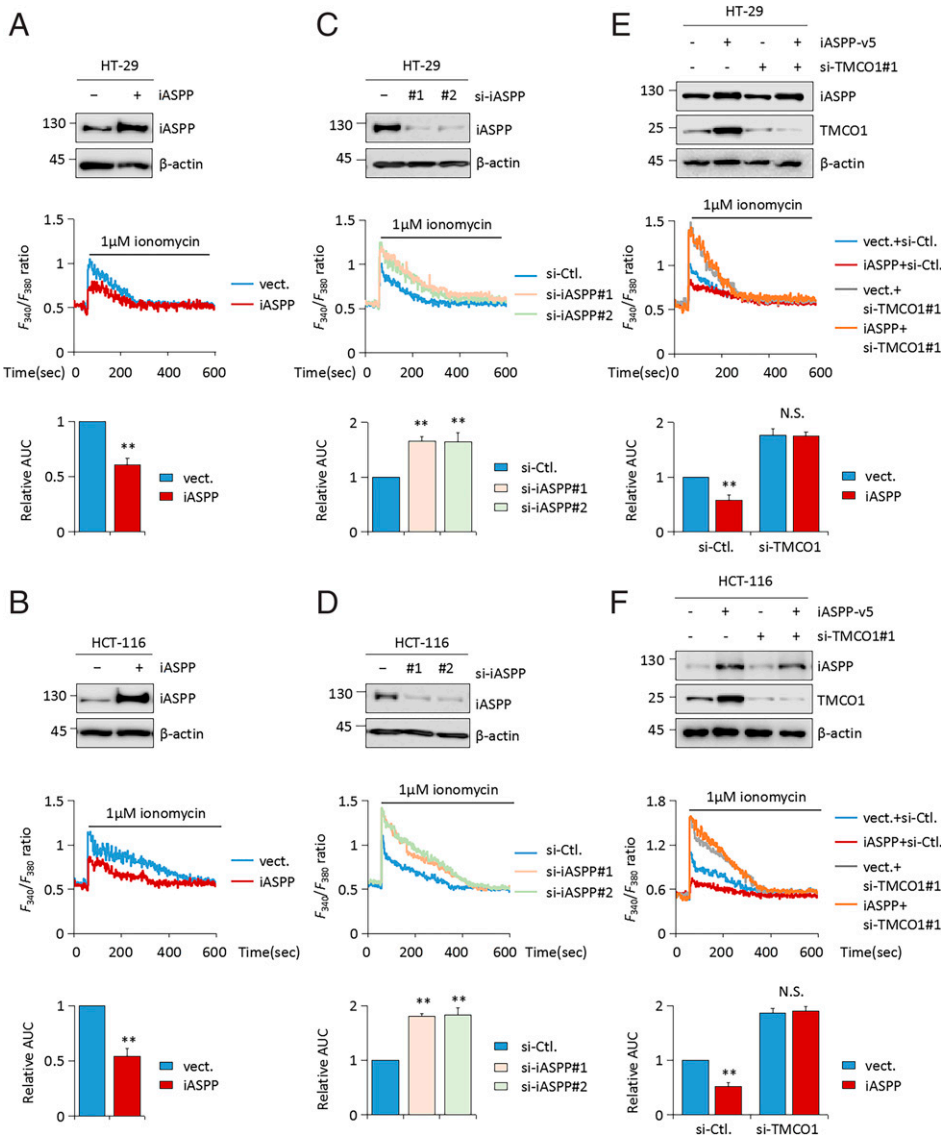

Fig. 6. Ca^{2+}-channel protein TMCO1 is required for the regulation of ER Ca^{2+} content by iASPP. (*A–F*) Representative WB images showing the efficiency of iASPP OE (*A* and *B*), KD (*C* and *D*), iASPP OE, or/and TMCO1 KD (*E* and *F*) in HT-29 and HCT-116 cells. β-actin was used as a loading control. ER Ca^{2+} stores in HT-29 (n = 20) and HCT-116 (n = 20) cells were measured by loading with 5 μM Fura-2 AM, following ionomycin (1 μM) in Ca^{2+}-free medium. The quantification of AUC derived from at least three independent experiments are presented as mean ± SEM in the bar graph at *Bottom*. Values in control cells were normalized to 1. $*P < 0.05$; $**P < 0.01$; N.S., not significant (*A–F*).

TMCO1 KD dramatically reduced colony formation of HT-29 and HCT-116 cells in a soft agar assay (Fig. 7*A*). iASPP KD elicited a similar effect (Fig. 7*A*), while there was no further reduction upon their combination (Fig. 7*A*).

The effects of iASPP-TMCO1 on tumor growth were also evaluated in vivo using a nude mouse xenograft model. The same numbers of HT-29 cells with different expression levels of iASPP and/or TMCO1 were inoculated into nude mice. Remarkably, either iASPP or TMCO1 KD reduced tumor growth and weight (Fig. 7 *B* and *C*). The effect of iASPP was largely diminished by TMCO1 KD (Fig. 7 *B* and *C*). There were no obvious changes in body weight in the different xenograft inoculated mouse models (Fig. 7*D*). In agreement with the in vitro data, we found that TMCO1 was reduced in iASPP KD xenografts (Fig. 7*E*). In line with the roles of iASPP/TMCO1 in regulating tumor growth, apoptosis rate, as indicated by cleaved caspase 3/7, was increased by iASPP and TMCO1 KD, and no further induction was observed with double KD (Fig. 7*F*).

iASPP-TMCO1 Axis Blunts Apoptotic Ca^{2+} Signals. Mounting evidence has suggested that some chemotherapeutic drugs act by disrupting Ca^{2+} homeostasis (43). We therefore further investigate the effects of iASPP-TMCO1 axis on the sensitivity of Ca^{2+}-related apoptosis. Toward this end, the apoptosis rates of iASPP or TMCO1 KD cells and their matched controls were examined before and after triggering Ca^{2+} release from the ER by TG or histamine treatment. As expected, apoptotic levels, as indicated by caspase 3/7 activities and Annexin V–positive rates, were increased by prolonged treatment with TG or histamine for 24 h (Fig. 8 *A* and *B*). Consistently, the percentages of Annexin V–positive apoptotic cells in iASPP or TMCO1 KD cells were much higher than in controls, under both unstressed and TG- or histamine-treated conditions (Fig. 8 *A* and *B*). By contrast, TMCO1 OE inhibits apoptosis (*SI Appendix*, Fig. S8*A*). Intriguingly, pretreatment of BAPTA-AM (BAPTA–acetoxymethyl ester) to chelate cytosolic Ca^{2+} abolished the effect of TG- and histamine-induced cell death, suggesting their effect is largely relying on the increased cytosolic Ca^{2+} (Fig. 8 *A* and *B*). Similar results were obtained in cells treated with staurosporine, a widely used chemotherapeutic drug (44) that has been reported to induce Ca^{2+}-dependent apoptosis (Fig. 8 *A* and *B*). Supportively, cytosolic Ca^{2+} was increased by drug treatments and TMCO1 KD augmented above effects, while BAPTA-AM completely abolished Ca^{2+} increase (*SI Appendix*, Fig. S8*B*). Staurosporine elevated cytosolic Ca^{2+} but not ER Ca^{2+} content (*SI Appendix*, Fig. S8 *B* and *C*). However, under treatment with the Ca^{2+}-independent apoptosis inducer etoposide (45), iASPP KD promoted apoptosis sensitivity

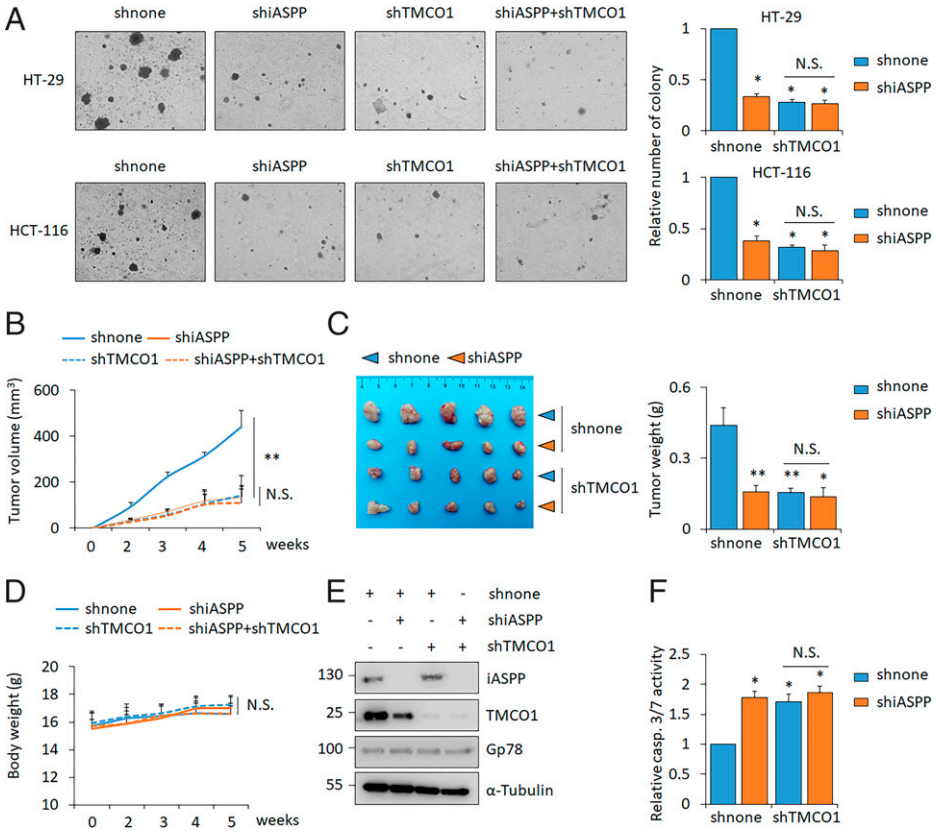

Fig. 7. iASPP-TMCO1 promote tumor growth both in vitro and in vivo. (*A*) Clone formation of HT-29 or HCT-116 stable lines infected with lentivirus expressing scrambled shRNA (shnone), shiASPP, shTMCO1, or shiASPP+shTMCO1. Relative clone formation ability was quantified and shown in bar graph with shnone normalized to 1. (*B–D*) Tumor volumes at the indicated time (*B*), tumor images (*C*), and tumor weight (*C*) of HT-29 xenografts and the body weights of nude mice (*D*) were presented. The average values are present in the graphs (means ± SD) (n = 5 for each pair). (*E* and *F*) The representative images of iASPP, TMCO1, and Gp78 proteins (*E*) and caspase 3/7 activity (*F*) were determined in the indicated xenografts. β-actin was used as a loading control. Bar graphs represent the mean ± SEM from three independent assays (*A* and *F*). *$P < 0.05$; **$P < 0.01$; N.S. not significant (*A–D*, *F*).

regardless of TMCO1 KD (Fig. 8 *A* and *B*). By soft agar assay, the same results were also observed. Namely, iASPP KD dramatically inhibited colony formation of HT-29 cells under the treatment of staurosporine. TMCO1 KD showed a similar effect, but double KD of iASPP and TMCO1 produced no further reduction (Fig. 8*C*). Calpains are known effectors of cytosolic Ca^{2+}-mediated apoptosis (46). Despite having no obvious impacts on calpain 1 (CAPN1) expression, iASPP OE decreased and iASPP KD increased calpain activities (*SI Appendix*, Fig. S8*D*). Calpain inhibitor, PD150606, abolished the effect of iASPP KD on both apoptosis and caspase-3/7 activation (*SI Appendix*, Fig. S8 *E* and *F*). These data suggest that iASPP regulates Ca^{2+}-regulated apoptosis by reducing calpain activities.

We further validated the roles of iASPP-TMCO1 in vivo in the HT-29 xenograft model. Staurosporine inhibited tumor growth, and iASPP KD or TMCO1 KD alone sensitized HT29 xenograft's response to staurosporine. However, double KD failed to produce additional effects (Fig. 8 *D–F*). There were no obvious body weight changes in the different mice models (*SI Appendix*, Fig. S7). These data suggest that iASPP and TMCO1 regulates the sensitivity to staurosporine by similar mechanism. In addition, iASPP KD and TMCO1-KD efficiency was confirmed by WB of xenografts. We also validated that iASPP KD reduced TMCO1 expression (Fig. 8*G*). Consistently, staurosporine-induced apoptosis, as indicated by the caspases 3/7 activity, was increased by inhibiting either iASPP or TMCO1. No further induction was observed with their combination (Fig. 8*H*). These data collectively suggest that inhibition of the iASPP-TMCO1 axis sensitizes cancer cells to Ca^{2+}-regulated cell death.

Discussion

Although Ca^{2+} deregulation has long been dismissed as a bystander of cancer development and resistance to therapy, accumulating preclinical and clinical evidence has supported a central role for alterations in Ca^{2+} homeostasis over recent years (2, 47). As such, Ca^{2+} homeostasis has begun to attract attention as a potential target for the development of novel anticancer therapies (2). However, Ca^{2+}-dependent changes in cell function are highly context specific, which made it a challenge to delineate their role in cancer.

In this report, we demonstrate that a recently identified Ca^{2+}-channel protein, TMCO1 is up-regulated in COAD at protein levels but not at mRNA levels. Further study revealed that TMCO1 is a substrate of E3 ligase Gp78. Intriguingly, the activity of Gp78-mediated TMCO1 degradation is under the control of oncogene iASPP. Mechanistically, iASPP promotes TMCO1 protein stability by competitively binding with Gp78, thus preventing Gp78-mediated TMCO1 degradation. Inhibition of iASPP-TMCO1 expression leads to increased sensitivity to Ca^{2+} signals of apoptosis (Fig. 8*I*). Furthermore, positive association between iASPP and TMCO1 expression is observed in vivo in human colon cancer tissues, further highlighting the significance of iASPP-TMCO1 in the pathogenesis of COAD.

The critical role of TMCO1 in modulating Ca^{2+} homeostasis was demonstrated in a recent study (12). Since then, TMCO1 has similarly been demonstrated to be involved in regulating osteoblast functions and ovarian follicle development (30, 48). However, whether or not it is associated with cancer has remained unclear. The identification of a positive association between the expression of the iASPP oncogene and TMCO1 suggests that TMCO1, like many other Ca^{2+} modulators, may contribute to the development of cancer. Indeed, TMCO1 levels are frequently elevated in human colon cancer tissues compared with adjacent normal controls. Increased TMCO1 is associated with advanced stages of colon cancer. Suppressing TMCO1 expression via genetic strategies promotes the occurrence of apoptosis. Additionally, TMCO1 inhibition leads to reduced tumor growth both in vitro in soft agar and in vivo in nude mice. In such contexts, altered expression of TMCO1 might

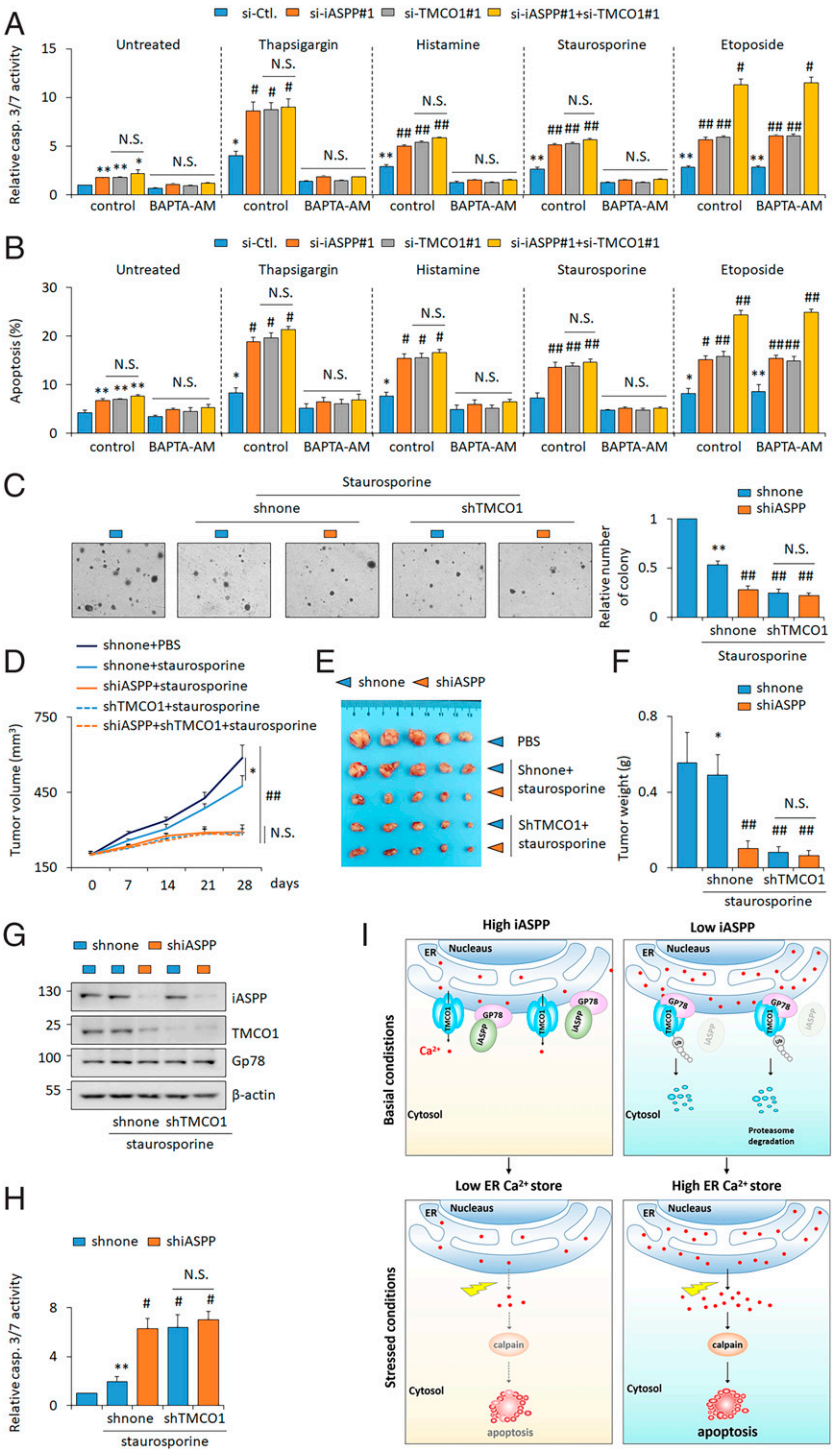

Fig. 8. Inhibiting iASPP-TMCO1 axis increases staurosporine sensitivity both in vitro and in vivo. (*A* and *B*) The apoptosis levels were revealed by caspase 3/7 activity assay (*A*) and Annexin V/PI staining (*B*) after iASPP KD, TMCO1 KD, or double KD in the presence of thapsigargin (1 μM), histamine (100 μM), staurosporine (100 nM), or etoposide (10 μM), with or without a selective calcium chelator BAPTA-AM (50 μM) in HT-29 cells. (*C*) Clone formation of shnone, shiASPP, shTMCO1, and shiASPP+shTMCO1 HT-29 stable lines with or without staurosporine (100 nM) was determined by soft agar assays. Relative clone formation ability was quantified and shown in the bar graph. The clone formation of the dimethyl sulfoxide (DMSO)–treated shnone HT-29 cells was normalized to 1. (*D–F*) Tumor volumes at the indicated time (*D*), tumor images (*E*), and the tumor weight (*F*) of the indicated HT-29 xenografts with or without staurosporine treatments were presented. (*G* and *H*) The representative images of iASPP, Gp78, and TMCO1 protein (*G*) and caspase 3/7 activity (*H*) were determined in the indicated xenografts. β-actin was used as a loading control. (*I*) Proposed model of iASPP's activity in regulating ER Ca^{2+} store by disrupting Gp78-mediated TMCO1 degradation. iASPP OE in cancer cells leads to an increased TMCO1 expression by competing with TMCO1 in binding with E3 ligase Gp78. The activation of the identified iASPP-Gp78/TMCO1 axis results in a decreased ER Ca^{2+} store, rendering cancer cells resistant to cytosolic Ca^{2+}-induced cell death. Cells with low iASPP expression levels or inhibiting iASPP expression sensitivities cell's response to cytosolic Ca^{2+}-induced cell death. Bar graphs represent the mean ± SEM from three independent assays (*A–C*). The average values are present in the graphs (*D*, *F*, and *H*) (means ± SD) ($n = 5$ for each group). $^{*}P < 0.05$; $^{**}P < 0.01$; N.S. not significant; $^{\#}P < 0.05$, $^{\#\#}P < 0.01$, compared with TG, histamine, staurosporine, or etoposide-treated controls (*A–D*, *F*, *H*).

be an adaptive response or might offer a survival advantage by inducing resistance to apoptosis. Controversially, Chien-Feng Li et al. recently claimed a tumor-suppressive role for TMCO1 in urinary bladder urothelial carcinoma (49). The discrepancy may be explained by different tissue contexts between colon cancers and bladder carcinomas. This idea matches the observations that both Ca^{2+}-channel inhibitors and antagonists are able to inhibit tumor growth in a cell context–dependent manner (50). Indeed, cytosolic Ca^{2+} is required for cell proliferative signaling, while Ca^{2+} overload leads to cell death (46, 51, 52). Understanding which Ca^{2+} channels, pumps, or even exchangers are altered in a particular cancer and their roles will aid their exploitation to kill cancer cells. In addition, Chien-Feng Li et al. have shown that TMCO1 inhibits tumors by recruiting PHLPP2 (PH domain and Leucine rich repeat Protein Phosphatase 2) to dephosphorylate Akt (49). It is not clear whether this is related to the remodeling of Ca^{2+} homeostasis. Whether TMCO1 has ER-Ca^{2+}–independent tumor-suppressor activity and under which circumstance this is the case remain to be elucidated.

It is also noteworthy that genetic inhibition of the iASPP-TMCO1 axis sensitizes cells under both unstressed conditions and treatment with reagents or chemotherapeutics that have been shown to disturb Ca^{2+} homeostasis. These results indicate that the iASPP-TMCO1 axis is not just a marker but also a

target that offers single or adjuvant therapeutic opportunities. Cancer cells with iASPP/TMCO1 OE have less intracellular Ca^{2+} for release from the ER upon activation of IP3R or other treatment-induced Ca^{2+} overload, resulting in apoptosis resistance. Such evidence is in keeping with previous work (53, 54) and supports the idea that modulation of Ca^{2+} homeostasis is a critical step in the regulation of cell responses to stress conditions and favors drug resistance in cancer.

Another important discovery of this study is the regulatory mechanism of TMCO1, which is mediated by E3 ligase Gp78. We provide solid evidence that TMCO1 is a substrate of Gp78 and that its levels can be modulated by Gp78. Notably, disruption Ca^{2+} homeostasis leads to ER stress coping response, such as the activation of ERAD. ERAD serves to degrade ER-associated misfolded or unassembled proteins, alleviating ER stress and facilitating adaptive survival. However, ERAD also targets folded functional proteins (55). Gp78 is an intrinsic ERAD ubiquitin E3 ligase (56), and TMCO1 serves as a functional substrate of ERAD, suggesting that cells may control ER stress by maintaining Ca^{2+} homeostasis through ERAD pathways. However, there was no association between Gp78 and TMCO1 in clinical samples. A potential explanation is that other E3 ligases may contribute to TMCO1 degradation. In support of this, in addition to Gp78, we found that RNF185 and RNF5 were able to reduce TMCO1 protein levels, possibly by indirect mechanisms, because they were not found to bind with TMCO1 in our experimental system. Alternatively, Gp78-mediated TMCO1 degradation is subjected to additional layers of regulation, such as the presence of oncogenic iASPP, as demonstrated here. Our data suggest that iASPP may be more important in controlling TMCO1 protein levels because a positive association between iASPP and TMCO1 was identified in our clinical samples. This may be because the presence of Gp78 is sufficient for TMCO1 degradation in cancer cells. Its activity in regulating its substrate TMCO1 is controlled by additional factors, such as iASPP. Thus, modulation of TMCO1's activity and expression by targeting the interaction of iASPP Gp78 may enable the development of a new kind of targeted anticancer therapy. Furthermore, Gp78's activity has been shown to be regulated by ubiquitin-specific protease 13 (USP13), a Ring domain binding protein with the deubiquitination enzyme activity (57). iASPP-regulated Gp78 inhibition identified in this study represents an alternative mechanism by which an oncogene is directly involved in regulating Gp78's binding with its substrate.

iASPP is an oncogene that has been shown to directly interact with p53. Such interaction is unlikely to occur in the cytosol as iASPP forms dimers there, which simultaneously block its p53 binding sites (33, 58). Therefore, iASPP regulates Ca^{2+} homeostasis independently of p53, although a previous study has found that p53 regulates Ca^{2+} signaling via its cytosolic activity elicited from the ER and/or mitochondria (59). Similarly, despite the robust effect of iASPP in regulating the antioxidative activity of Nrf2 and the clear involvement of Nrf2 in regulating Ca^{2+} homeostasis, iASPP regulates Ca^{2+} homeostasis independently of Nrf2. Of note, Nrf2 mainly regulates Ca^{2+} homeostasis by modulating the redox-sensitive transient receptor potential cation channel (60). Additional work is urgently needed to disentangle the role of iASPP in regulating the cross talk between oxidative stress and Ca^{2+} homeostasis. In addition, we found that iASPP/TMCO1-induced apoptosis is mainly dependent on the cytosolic Ca^{2+} signal because cytosolic chelator BAPTA-AM largely abolished the treatment-induced cell death. However, we cannot exclude the involvement of mitochondria, as mitochondria and ER are functionally and physically associated (61).

In summary, our data highlight key examples of a Ca^{2+}-channel protein that is involved in the development of cancer and an oncogene that modulates Ca^{2+} homeostasis. We demonstrate the biochemical mechanism of iASPP-regulated Gp78-mediated TMCO1 degradation, which causes deregulated Ca^{2+} homeostasis and increased resistance to increased Ca^{2+}-triggered apoptosis in cancer cells. These findings suggest the future potential of the development of pharmacological or genetic approaches for the treatment of cancer by modulating Ca^{2+} homeostasis.

Materials and Methods

Cell Lines and Transfection. The human colorectal cancer cell line HCT-15, SW480, SW620, COLO 205, HCT-116, HT-29, and the lung cancer cell line H1299 had been authenticated and characterized by the supplier. The detailed culture conditions, transfection methods, and siRNA sequences used in this study can be found in *SI Appendix, Supplementary Materials and Methods*.

Colon Cancer Patient Samples. A total of 40 pairs human colorectal cancer tissues and their corresponding adjacent normal controls were collected from the Third Affiliated Hospital of Harbin Medical University in China. Written informed consent was obtained from all patients. All samples were obtained and stored in liquid nitrogen immediately after surgery. The study has been approved by the Research Ethics Committee of Harbin Medical University, China.

Other Methods. RNA extraction and qRT-PCR, WB assay, measurement of Ca^{2+} flux, in vitro translation, purification of recombinant protein, IP assay, ubiquitination assay, apoptosis assay, caspase 3/7 activity assay, clonogenic survival assay, in vivo xenografted tumor model, calpain activity assay, mass spectrum, and statistical analysis can be found in *SI Appendix, Supplementary Materials and Methods*.

Data Availability. All study data are included in the article and/or *SI Appendix*.

ACKNOWLEDGMENTS. We thank Professor Ronggui Hu from Shanghai Institute of Biochemistry and Cell Biology for kindly providing hemagglutinin-Ubiquitins and a catalytic core domain of the USP2 deubiquitinase (USP2cc). This work was funded by the National Nature Science Foundation of China (No. 82025027, 31871389, 31741084, 32000517, 82030033, and 91754204) and China Postdoctoral Science Foundation (No. 2020M680045 and 2021T140161) and the Nature Science Foundation of Heilongjiang Province (No. YQ2021C024).

1. D. Hanahan, R. A. Weinberg, Hallmarks of cancer: The next generation. *Cell* **144**, 646–674 (2011).
2. S. Marchi, C. Giorgi, L. Galluzzi, P. Pinton, Ca^{2+} fluxes and cancer. *Mol. Cell* **78**, 1055–1069 (2020).
3. J. Chen, A. Sitsel, V. Benoy, M. R. Sepúlveda, P. Vangheluwe, Primary active Ca^{2+} transport systems in health and disease. *Cold Spring Harb. Perspect. Biol.* **12**, a035113 (2020).
4. M. J. Berridge, M. D. Bootman, H. L. Roderick, Calcium signalling: Dynamics, homeostasis and remodelling. *Nat. Rev. Mol. Cell Biol.* **4**, 517–529 (2003).
5. A. Raffaello, C. Mammucari, G. Gherardi, R. Rizzuto, Calcium at the center of cell signaling: Interplay between endoplasmic reticulum, mitochondria, and lysosomes. *Trends Biochem. Sci.* **41**, 1035–1049 (2016).
6. R. G. Efremov, A. Leitner, R. Aebersold, S. Raunser, Architecture and conformational switch mechanism of the ryanodine receptor. *Nature* **517**, 39–43 (2015).
7. R. Zalk, A. R. Marks, Ca^{2+} release channels join the 'resolution revolution'. *Trends Biochem. Sci.* **42**, 543–555 (2017).
8. K. Hamada, K. Mikoshiba, IP_3 receptor plasticity underlying diverse functions. *Annu. Rev. Physiol.* **82**, 151–176 (2020).
9. E. R. Chemaly, L. Troncone, D. Lebeche, SERCA control of cell death and survival. *Cell Calcium* **69**, 46–61 (2018).
10. P. B. Stathopulos *et al.*, STIM1/Orai1 coiled-coil interplay in the regulation of store-operated calcium entry. *Nat. Commun.* **4**, 2963 (2013).
11. C. Y. Park *et al.*, STIM1 clusters and activates CRAC channels via direct binding of a cytosolic domain to Orai1. *Cell* **136**, 876–890 (2009).
12. Q.-C. Wang *et al.*, TMCO1 is an ER Ca(2+) load-activated Ca(2+) channel. *Cell* **165**, 1454–1466 (2016).
13. N. Prevarskaya, R. Skryma, Y. Shuba, Calcium in tumour metastasis: New roles for known actors. *Nat. Rev. Cancer* **11**, 609–618 (2011).

14. H. L. Roderick, S. J. Cook, Ca^{2+} signalling checkpoints in cancer: Remodelling Ca^{2+} for cancer cell proliferation and survival. *Nat. Rev. Cancer* **8**, 361–375 (2008).
15. S. Kuchay *et al.*, PTEN counteracts FBXL2 to promote IP3R3- and Ca^{2+}-mediated apoptosis limiting tumour growth. *Nature* **546**, 554–558 (2017).
16. G. Roti *et al.*, Complementary genomic screens identify SERCA as a therapeutic target in NOTCH1 mutated cancer. *Cancer Cell* **23**, 390–405 (2013).
17. A. Bononi *et al.*, BAP1 regulates IP3R3-mediated Ca^{2+} flux to mitochondria suppressing cell transformation. *Nature* **546**, 549–553 (2017).
18. M. Feng *et al.*, Store-independent activation of Orai1 by SPCA2 in mammary tumors. *Cell* **143**, 84–98 (2010).
19. A. Nougarede *et al.*, Breast cancer targeting through inhibition of the endoplasmic reticulum-based apoptosis regulator Nrh/BCL2L10. *Cancer Res.* **78**, 1404–1417 (2018).
20. S. Yang, J. J. Zhang, X.-Y. Huang, Orai1 and STIM1 are critical for breast tumor cell migration and metastasis. *Cancer Cell* **15**, 124–134 (2009).
21. N. Yang *et al.*, Blockade of store-operated Ca(2+) entry inhibits hepatocarcinoma cell migration and invasion by regulating focal adhesion turnover. *Cancer Lett.* **330**, 163–169 (2013).
22. J. Xia *et al.*, Elevated Orai1 and STIM1 expressions upregulate MACC1 expression to promote tumor cell proliferation, metabolism, migration, and invasion in human gastric cancer. *Cancer Lett.* **381**, 31–40 (2016).
23. P. Ueasilamongkol *et al.*, Type 3 inositol 1,4,5-trisphosphate receptor is increased and enhances malignant properties in cholangiocarcinoma. *Hepatology* **71**, 583–599 (2020).
24. W. Zhao *et al.*, 1B50-1, a mAb raised against recurrent tumor cells, targets liver tumor-initiating cells by binding to the calcium channel $\alpha 2\delta 1$ subunit. *Cancer Cell* **23**, 541–556 (2013).
25. F. Zhong *et al.*, Induction of Ca^{2+}-driven apoptosis in chronic lymphocytic leukemia cells by peptide-mediated disruption of Bcl-2-IP3 receptor interaction. *Blood* **117**, 2924–2934 (2011).
26. L. Pagliaro, M. Marchesini, G. Roti, Targeting oncogenic Notch signaling with SERCA inhibitors. *J. Hematol. Oncol.* **14**, 8 (2021).
27. K. P. Burdon *et al.*, Genome-wide association study identifies susceptibility loci for open angle glaucoma at TMCO1 and CDKN2B-AS1. *Nat. Genet.* **43**, 574–578 (2011).
28. D. Pehlivan *et al.*, Centers for Mendelian Genomics, Whole-exome sequencing links TMCO1 defect syndrome with cerebro-facio-thoracic dysplasia. *Eur. J. Hum. Genet.* **22**, 1145–1148 (2014).
29. Y. Alanay *et al.*, TMCO1 deficiency causes autosomal recessive cerebrofaciothoracic dysplasia. *Am. J. Med. Genet. A.* **164A**, 291–304 (2014).
30. J. Li *et al.*, TMCO1-mediated Ca^{2+} leak underlies osteoblast functions via CaMKII signaling. *Nat. Commun.* **10**, 1589 (2019).
31. B. Xin *et al.*, Homozygous frameshift mutation in TMCO1 causes a syndrome with craniofacial dysmorphism, skeletal anomalies, and mental retardation. *Proc. Natl. Acad. Sci. U.S.A.* **107**, 258–263 (2010).
32. C. Giorgi, A. Danese, S. Missiroli, S. Patergnani, P. Pinton, Calcium dynamics as a machine for decoding signals. *Trends Cell Biol.* **28**, 258–273 (2018).
33. M. Lu *et al.*, Restoring p53 function in human melanoma cells by inhibiting MDM2 and cyclin B1/CDK1-phosphorylated nuclear iASPP. *Cancer Cell* **23**, 618–633 (2013).
34. H. Li *et al.*, A previously identified apoptosis inhibitor iASPP confers resistance to chemotherapeutic drugs by suppressing senescence in cancer cells. *J. Biol. Chem.* **295**, 4049–4063 (2020).
35. W. Ge *et al.*, iASPP is an antioxidative factor and drives cancer growth and drug resistance by competing with Nrf2 for Keap1 binding. *Cancer Cell* **32**, 561–573.e6 (2017).
36. B. Lu *et al.*, Increased expression of iASPP, regulated by hepatitis B virus X protein-mediated NF-κB activation, in hepatocellular carcinoma. *Gastroenterology* **139**, 2183–2194.e5 (2010).
37. L. Jiang *et al.*, iASPP and chemoresistance in ovarian cancers: Effects on paclitaxel-mediated mitotic catastrophe. *Clin. Cancer Res.* **17**, 6924–6933 (2011).
38. G. Trigiante, X. Lu, ASPP [corrected] and cancer. *Nat. Rev. Cancer* **6**, 217–226 (2006).
39. K. N. Swatek, D. Komander, Ubiquitin modifications. *Cell Res.* **26**, 399–422 (2016).
40. L. Wen *et al.*, iASPP-mediated ROS inhibition drives 5-Fu resistance dependent on Nrf2 antioxidative signaling pathway in gastric adenocarcinoma. *Dig. Dis. Sci.* **65**, 2873–2883 (2020).
41. K.-K. Chan *et al.*, Overexpression of iASPP is required for autophagy in response to oxidative stress in choriocarcinoma. *BMC Cancer* **19**, 953 (2019).
42. K. Liu *et al.*, Wild-type and mutant p53 differentially modulate miR-124/iASPP feedback following pohotodynamic therapy in human colon cancer cell line. *Cell Death Dis.* **8**, e3096 (2017).
43. W.-T. Kuo *et al.*, Inflammation-induced occludin downregulation limits epithelial apoptosis by suppressing caspase-3 expression. *Gastroenterology* **157**, 1323–1337 (2019).
44. J. Chandra *et al.*, Resistance of leukemic cells to 2-chlorodeoxyadenosine is due to a lack of calcium-dependent cytochrome c release. *Blood* **99**, 655–663 (2002).
45. C. E. Steuer *et al.*, Comparison of concurrent use of thoracic radiation with either carboplatin-paclitaxel or cisplatin-etoposide for patients with stage III non-small-cell lung cancer: A systematic review. *JAMA Oncol.* **3**, 1120–1129 (2017).
46. J. Fang *et al.*, A calcium- and calpain-dependent pathway determines the response to lenalidomide in myelodysplastic syndromes. *Nat. Med.* **22**, 727–734 (2016).
47. M. J. Berridge, P. Lipp, M. D. Bootman, The versatility and universality of calcium signalling. *Nat. Rev. Mol. Cell Biol.* **1**, 11–21 (2000).
48. Z. Sun *et al.*, TMCO1 is essential for ovarian follicle development by regulating ER Ca^{2+} store of granulosa cells. *Cell Death Differ.* **25**, 1686–1701 (2018).
49. C.-F. Li *et al.*, Transmembrane and coiled-coil domain 1 impairs the AKT signaling pathway in urinary bladder urothelial carcinoma: A characterization of a tumor suppressor. *Clin. Cancer Res.* **23**, 7650–7663 (2017).
50. C. Cui, R. Merritt, L. Fu, Z. Pan, Targeting calcium signaling in cancer therapy. *Acta Pharm. Sin. B* **7**, 3–17 (2017).
51. S. P. Chelko *et al.*, Exercise triggers CAPN1-mediated AIF truncation, inducing myocyte cell death in arrhythmogenic cardiomyopathy. *Sci. Transl. Med.* **13**, eabf0891 (2021).
52. L. Scorrano *et al.*, BAX and BAK regulation of endoplasmic reticulum Ca^{2+}: A control point for apoptosis. *Science* **300**, 135–139 (2003).
53. F. Vanden Abeele *et al.*, Bcl-2-dependent modulation of Ca(2+) homeostasis and store-operated channels in prostate cancer cells. *Cancer Cell* **1**, 169–179 (2002).
54. C. White *et al.*, The endoplasmic reticulum gateway to apoptosis by Bcl-X(L) modulation of the InsP3R. *Nat. Cell Biol.* **7**, 1021–1028 (2005).
55. J. C. Christianson, Y. Ye, Cleaning up in the endoplasmic reticulum: Ubiquitin in charge. *Nat. Struct. Mol. Biol.* **21**, 325–335 (2014).
56. B.-L. Song, N. Sever, R. A. DeBose-Boyd, Gp78, a membrane-anchored ubiquitin ligase, associates with Insig-1 and couples sterol-regulated ubiquitination to degradation of HMG CoA reductase. *Mol. Cell* **19**, 829–840 (2005).
57. Y. Liu *et al.*, USP13 antagonizes gp78 to maintain functionality of a chaperone in ER-associated degradation. *eLife* **3**, e01369 (2014).
58. M. Lu *et al.*, A code for RanGDP binding in ankyrin repeats defines a nuclear import pathway. *Cell* **157**, 1130–1145 (2014).
59. C. Giorgi *et al.*, p53 at the endoplasmic reticulum regulates apoptosis in a Ca^{2+}-dependent manner. *Proc. Natl. Acad. Sci. U.S.A.* **112**, 1779–1784 (2015).
60. J. Weerachayaphorn *et al.*, Nuclear factor, erythroid 2-like 2 regulates expression of type 3 inositol 1,4,5-trisphosphate receptor and calcium signaling in cholangiocytes. *Gastroenterology* **149**, 211–222.e10 (2015).
61. G. Csordás, D. Weaver, G. Hajnóczky, Endoplasmic reticulum-mitochondrial contactology: Structure and signaling functions. *Trends Cell Biol.* **28**, 523–540 (2018).